Heteroatom Chemistry
Volume 12, Number 4, 2001

Syntheses and Structural Characterization of Water-Soluble Selenium Reagents for the Redox Control of Protein Disulfide Bonds

Michio Iwaoka, Taro Takahashi, and Shuji Tomoda

Department of Life Sciences, Graduate School of Arts and Sciences, The University of Tokyo, Komaba, Meguro-ku, Tokyo 153-8902, Japan; E-mail: tomoda@selen.c.u-tokyo.ac.jp

Received 18 December 2000; revised 18 January 2001

ABSTRACT: *A new class of water-soluble redox reagents (***1–4***) that contain selenium as the active site was developed for the purpose of the redox control of protein structures. The X-ray crystallographic analyses revealed that trans-3,4-dihydroxy-1-selenolane (DHS*^{red}*) (***1***) and its Se-oxide (DHS*^{ox}*) (***2***) have two axial hydroxy groups on the selenolane five-membered ring, whereas trans-1,2-diselenane-4,5-diol (DST*^{ox}*) (***3***), a selenium analog of oxidized dithiothreitol (DTT*^{ox}*), has two equatorial hydroxy groups on the diselenane six-membered ring. According to the vicinal* $^3J_{HH}$ *coupling constants observed for* **1–3***, it was suggested that they adopt similar structures in solution to those in the solid state. Diselenothreitol (DST*^{red}*) (***4***), a selenium analog of dithiothreitol (DTT*^{red}*), was also synthesized, but it was too air sensitive to be isolated. The reactions of* **1–4** *with DTT*^{ox} *and DTT*^{red} *indicated that the oxidizing power of DHS*^{ox} *(***2***) exceeds by far that of DTT*^{ox}*, while the reducing power of DST*^{red} *(***4***) exceeds that of DTT*^{red}*.* © 2001 John Wiley & Sons, Inc. Heteroatom Chem 12:293–299, 2001

INTRODUCTION

Disulfide (SS) bonds in proteins are important elements for the conformational stability of the native folded state [1]. Proteins lose their native structure by cleavage of the SS bonds, but the native structure can be regenerated by formation of the SS bonds for small monomeric proteins [2]. In such cases, the protein structures can be reversibly controlled by reduction and oxidation of the SS bonds in vitro [3].

To control the redox states of protein SS bonds, organic sulfur reagents, such as glutathione (GSH) [4,5], dithiothreitol (DTT) [6,7], 2-mercaptoethanol [4,6], and cystamine [8] are usually employed in vivo and in vitro. However, since the redox power of these sulfur reagents is not reasonably strong, excess amounts of the reagents as well as a limited pH range are required to control protein structures by using such reagents. Barany et al. [9] recently developed novel solid-phase reagents for facile formation of peptide SS bonds. Although the active site of the reagents includes an SS functional group like the oxidized forms of normal sulfur reagents, the polymer support enables efficient formation of peptide SS bonds in a wide pH range. On the other hand, Shi and Rabenstein [10] reported that platinum complex *trans*-$[Pt(ethylenediamine)_2Cl_2]^{2+}$ is a highly selective and efficient reagent for the quantitative formation of intramolecular SS bonds in peptides. This reagent is different from previous redox reagents in that a transition metal is involved as the redox center.

Dedicated to Professor Naoki Inamoto on the occasion of his 72nd birthday.

Correspondence to: Shuji Tomoda.

Contract Grant Sponsor:
Contract Grant Number: Grant-in-Aid for Scientific Research 11740346.
Contract Grant Sponsor: Mitsubishi Chemical Corporation Fund.

We have recently developed a new class of redox reagents (DHS^{red}, **1**; DHS^{ox}, **2**) that contain redox-active selenium instead of sulfur [11]. The selenium reagents were designed on the basis of the observations that the redox activity of selenium is higher than that of sulfur [12] and that some selenium compounds work as good catalysts for the formation or the reduction of SS bonds in organic and enzyme-mimetic reactions [13]. According to the oxidative regeneration experiments of ribonuclease A having four intramolecular SS bonds, it was shown that **2** is a rapid and quantitative reagent for formation of SS bonds in polypeptides in a wide range of pH (at least from pH 3 to 9) [11].

In this article, synthesis and structural characterization of new water-soluble selenium reagents (**1–4**), which have been developed for the purpose of redox control of protein structures, are presented in detail [14]. Configurations and conformations of **1–3** were unambiguously determined in the solid state by X-ray analysis. According to the vicinal $^3J_{HH}$ coupling constants observed for **1–3**, it was suggested that their conformations in solution are similar to those in the solid state. The redox properties of **1–4** are also reported briefly on the basis of the reactions of **1–4** with sulfur reagents DTT^{ox} (**5**) and DTT^{red} (**6**).

RESULTS AND DISCUSSION

Synthesis

Following the synthetic procedure of DTT^{ox} (**5**) [15], a racemic mixture of 1,3-butadiene diepoxide was allowed to react with NaHSe or Na_2Se_2 in water (Schemes 1 and 2). Since the reaction products (*trans*-3,4-dihydroxy-1-selenolane [DHS^{red}, **1**] and *trans*-1,2-diselenane-4,5-diol [DST^{ox}, **3**], respectively) were soluble in both water and ether, continuous extraction with ether was necessary to isolate the products. Obtained **1** and **3** were stable at room temperature under air at least for a few months.

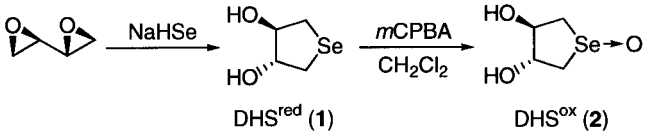

SCHEME 1

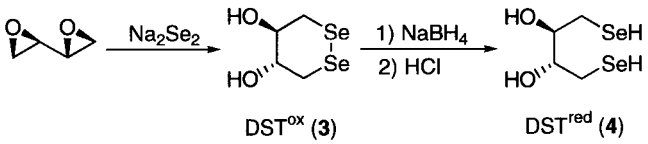

SCHEME 2

Treatment of DHS^{red} (**1**) with *m*-chloroperbenzoic acid in dichloromethane (CH_2Cl_2) generated the corresponding selenium oxide (DHS^{ox}) (**2**) as a colorless precipitate due to the low solubility of **2** in the solvent; **2** was stable at room temperature under air and was readily soluble in water. It should be noted that each hydrogen and carbon atom gives a different NMR signal in solution due to the chiral center at the selenium atom, except for the two hydroxy (OH) hydrogen atoms.

On the other hand, the reduction of DST^{ox} (**3**) with sodium borohydride ($NaBH_4$) followed by the addition of aqueous HCl afforded diselenothreitol (DST^{red}) (**4**) as a white powder. Compound **4** was too air sensitive to be isolated presumably due to the high reactivity of the selenol moieties: the crude product contained ~20% of an unknown byproduct (^{77}Se NMR δ −82.8). The open-chain diselenol structure of **4** was explicitly characterized by ^{1}H NMR [δ −0.51 (t, $^3J_{HH}$ = 7.5 Hz, SeH)] and ^{77}Se NMR [δ −78.3 (d, $^1J_{SeH}$ = 33.5 Hz)] spectroscopy. The observed value of $^1J_{SeH}$ was slightly smaller than the normal values of $^1J_{SeH}$ (~40 to ~65 Hz) [16], suggesting enhanced acidity of the selenol moieties of **4**.

Although the molecular formulae of **1–4** could be easily drawn based on the NMR and/or elemental analyses, their configurations (trans or cis) and conformations (axial or equatorial) as to the two OH substituents were not obvious only from the spectroscopic data. In order to clarify these structural features, X-ray crystallographic analysis was performed for **1–3**.

X-ray analysis

Molecular structures of DHS^{red} (**1**), DHS^{ox} (**2**), and DST^{ox} (**3**) determined by X-ray analysis are shown in Figures 1–3. All atoms including hydrogen atoms were reasonably located by the difference Fourier maps, and their atomic parameters were refined by the least-squares methods without constraints. As clearly seen in the figures, the two OH substituents are trans to each other for all cases, indicating that the reactions of 1,3-butadiene diepoxide with NaHSe and Na_2Se_2 (Schemes 1 and 2) proceeded with retention of configuration at C2 and C3. Thus the configurations of **1–3**, and hence that of DST^{red} (**4**), could be unambiguously determined.

Two crystallographically independent molecules are present for DHS^{red} (**1**), one of which is located at an equivalent position (Figure 1). The two molecules have similar conformations to each other with two axial OH substituents on the selenolane five-membered ring (O1–C2–C3–O2 = −171.2°, O3–C6–C6_2–O3_2 = 173.3°). Similarly, DHS^{ox} (**2**) exists as a diax-

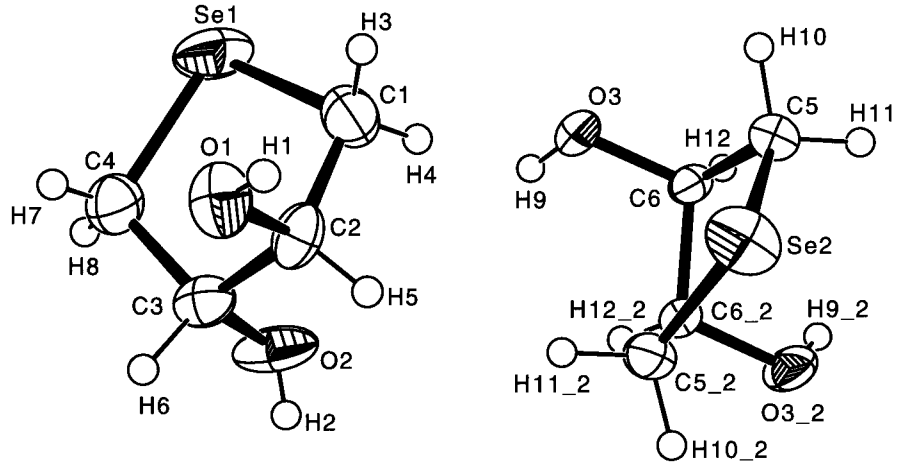

FIGURE 1 ORTEP plot for DHS^{red} (**1**) at the 50% probability level. Selected bond parameters: Se1–C1 1.953(5), Se1–C4 1.949(5), Se2–C5 1.959(4), O1–C2 1.428(5), O2–C3 1.429(5), O3–C6 1.421(5), C1–C2 1.515(6), C2–C3 1.516(6), C3–C4 1.495(6), C5–C6 1.515(6), C6–C6_2 1.526(7), C4–Se1–C1 89.4(2), C5–Se2–C5_2 89.9(3), C2–C1–Se1 106.9(3), C1–C2–C3 108.5(4), C4–C3–C2 108.3(4), C3–C4–Se1 106.5(3), C6–C5–Se2 106.4(3), C5–C6–C6–_2 108.6(2), C4–Se1–C1–C2 −9.8(3), Se1–C1–C2–C3 34.4(4), O1–C2–C3–O2 −171.2(3), C1–C2–C3–C4 −49.8(5), C2–C3–C4–Se1 40.0(4), C1–Se1–C4–C3 −16.8(4), C5_2–Se2–C5–C6 13.24(17), Se2–C5–C6–C6_2 −37.0(4), O3–C6–C6_2–O3_2 173.3(6), C5–C6–C6_2–C5_2 49.7(8).

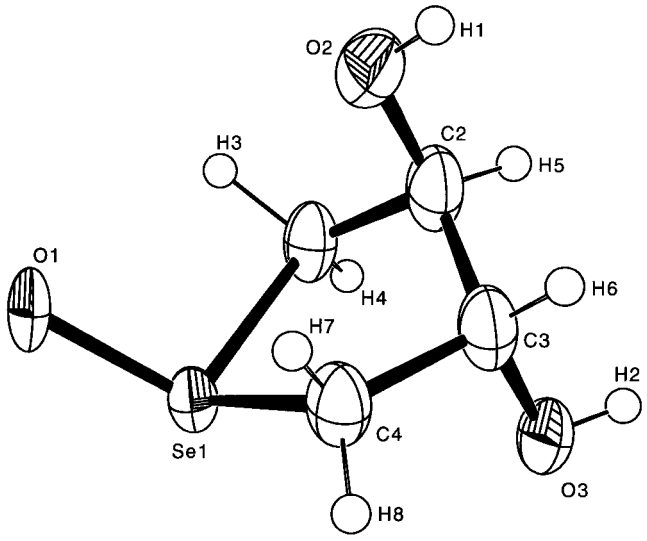

FIGURE 2 ORTEP plot for DHS^{ox} (**2**) at the 50% probability level. Selected bond parameters: Se1–O1 1.679(4), Se1–C1 1.946(6), Se1–C4 1.946(6), O2–C2 1.433(8), O3–C3 1.444(8), C1–C2 1.531(8), C2–C3 1.491(9), C3–C4 1.515(8), O1–Se1–C1 103.8(2), O1–Se1–C4 104.5(3), C1–Se1–C4 88.9(2), C2–C1–Se1 107.4(4), C3–C2–C1 107.2(5), C2–C3–C4 107.5(5), C3–C4–Se1 104.8(4), C4–Se1–C1–C2 −6.1(5), Se1–C1–C2–C3 33.5(6), O2–C2–C3–O3 179.4(4), C1–C2–C3–C4 −53.0(7), C2–C3–C4–Se1 46.3(6), C1–Se1–C4–C3 −21.9(5).

ial conformation as to the two OH substituents in the solid state (O2–C2–C3–O3 = 179.4°) (Figure 2). Although the relative stability of the diaxial and diequatorial conformations may depend on the substituents on the selenolane ring and the molecular packing in the solid state, it seems that the diaxial conformation is intrinsically more stable than the diequatorial one because diaxial conformations have been usually observed for analogous thiolane compounds in the solid state [17].

In contrast, DST^{ox} (**3**) has two equatorial OH substituents on the diselenane six-membered ring (O1–C2–C3–O2 = 53.2°), which adopts a slightly distorted chair conformation (Figure 3). The diequatorial conformation is stabilized by an intramolecular hydrogen bond (O1–H1 $\cdots$ O2; H1 $\cdots$ O2 2.38 Å, O1–H1 $\cdots$ O2 116°). A similar molecular structure has been reported for DTT^{ox} (**5**) in the solid state [18]. The bond parameters (bond lengths, bond angles, and dihedral angles) of the diselenane ring observed for **3** were entirely consistent with those reported for 1,2-diselenane-3,6-dicarboxylic acid [19].

Stable Conformations in Solution

Since the reactivity of a compound depends on the structure, it is important to elucidate a major conformation in solution. The structures observed for **1**–**3** in the solid state are needless to say strong candidates for the major conformations in solution although they are not necessary the same as those in the solid state.

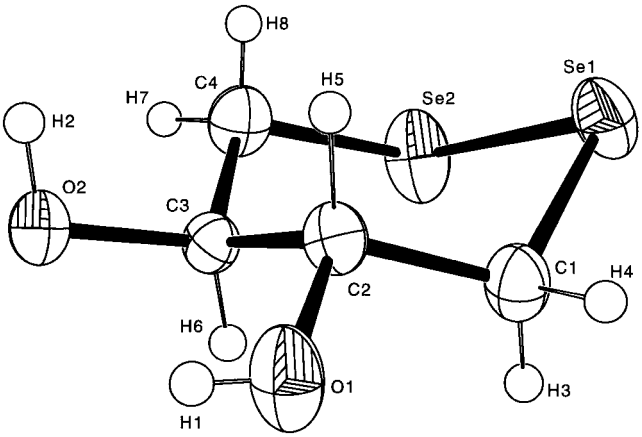

FIGURE 3 ORTEP plot for DST^{ox} (**3**) at the 50% probability level. Selected bond parameters: Se1–Se2 2.3108(9), Se1–C1 1.945(4), Se2–C4 1.947(4), O1–C2 1.442(5), O2–C3 1.435(4), C1–C2 1.514(5), C2–C3 1.518(5), C3–C4 1.521(5), O1 ··· O2 2.740(3), H1 ··· O2 2.38, C1–Se1–Se2 94.68(13), C4–Se2–Se1 95.90(14), C2–C1–Se1 113.3(3), C1–C2–C3 115.4(3), C2–C3–C4 115.1(3), C3–C4–Se2 113.0(3), O1–H1 ··· O2 116, C1–Se1–Se2–C4 53.93(19), Se2–Se1–C1–C2 −63.2(3), Se1–C1–C2–C3 69.8(4), O1–C2–C3–O2 53.2(4), C1–C2–C3–C4 −67.0(5), C2–C3–C4–Se2 68.0(4), Se1–Se2–C4–C3 −62.5(3).

The major conformations of **1–3** in solution were deducible from the observed *J* coupling constants between vicinal hydrogen atoms ($^3J_{HH}$) by using the Karplus equation [20]. For the case of DHS^{red} (**1**), the values of $^3J_{HH}$ for the CH–CH$_2$ moiety were 4.0 Hz and 4.0 Hz, suggesting that the HC–CH dihedral angles are ~60° or ~120°. Since the only possible dihedral angle is ~60°, both C–O bonds of **1** would be axial in the major conformation in solution. Similarly, for the case of DHS^{ox} (**2**), the values of $^3J_{HH}$ for the one CH–CH$_2$ moiety were 3.0 Hz and 2.5 Hz, and those for the other were 5.5 Hz and ~0 Hz: the two CH–CH$_2$ moieties exhibited different NMR behaviors due to the chiral center at the selenium atom. Possible combinations of the HC–CH dihedral angles are ~70° and ~70° for the former CH–CH$_2$ moiety and ~50° and ~90° for the latter one, suggesting that the major conformation of **2** in solution has axial C–O bonds. The observed value of $^3J_{HH}$ for the central CH–CH moiety of **2** (3.0 Hz) also supported this assignment. On the other hand, DST^{ox} (**3**) exhibited different behaviors: the values of $^3J_{HH}$ for CH–CH$_2$ were 10.0 Hz and 2.8 Hz, suggesting that the HC–CH dihedral angles are ~180° and ~70°. Therefore, the major conformation of **3** in solution would have equatorial C–O bonds.

According to the previous conformational analyses, it is suggested that the predominant conformations of **1–3** in solution are similar to those in the solid state. However, the two OH groups of **1–3** may freely rotate in solution or locate in different positions from those in the solid state.

Reactivity of DHS and DST

The redox reactivity of DHS^{red} (**1**) and DHS^{ox} (**2**) were tested by the reactions with DTT^{ox} (**5**) and DTT^{red} (**6**) in various buffer solutions (pH ~4.0–9.0) (Scheme 3). Reverse-phase high-performance liquid chromatography (HPLC) analysis of the mixtures of DHS^{red} (**1**) and DTT^{ox} (**5**) at various ratios (5:1 ~ 1:200) revealed that the forward reaction of Scheme 3 does not proceed at all under these conditions. On the other hand, the 1:1 mixture of DHS^{ox} (**2**) and DTT^{red} (**6**) rapidly produced DHS^{red} (**1**) and DTT^{ox} (**5**) quantitatively (within 10 seconds at room temperature). The results clearly showed that the oxidizing power of DHS^{ox} (**2**) by far exceeds that of DTT^{ox} (**5**). Indeed, the oxidation of the reduced form of ribonuclease A, which has eight SH groups along the polypeptide chain, with DHS^{ox} (**2**) was extremely faster than that with DTT^{ox} (**5**) [11].

Similarly, the redox reactivity of DST^{ox} (**3**) and DST^{red} (**4**) were tested by the reactions with DTT^{ox} (**5**) and DTT^{red} (**6**) (Scheme 4). Reverse-phase HPLC analysis of the mixtures of DST^{ox} (**3**) and DTT^{red} (**6**) at various ratios (1:1 ~ 1:100) revealed that the backward reaction of Scheme 4 does not proceed at all at pH values of ~4.0–9.0. On the other hand, NMR analysis of a mixture of DST^{red} (**4**) and DTT^{ox} (**5**) in D$_2$O showed facile formation of DST^{ox} (**3**) and DTT^{red} (**6**): according to the ^{1}H NMR spectrum, DST^{red} (**4**) disappeared completely to form DTT^{red} (**6**) within 5 minutes at room temperature. Therefore, the reducing power of DST^{red} (**4**) was found to be higher than that of DTT^{red} (**6**).

CONCLUSIONS

New water-soluble selenium reagents (**1–4**) were synthesized, and their structures were characterized in the solid state and also in solution. In the solid state, DHS^{red} (**1**) and DHS^{ox} (**2**) have two axial OH groups on the selenolane five-membered ring, whereas DST^{ox} (**3**) has two equatorial OH groups on the diselenane six-membered ring. Similar structures are probably the major conformations of **1–3** in solution. The reactions of **1–4** with DTT^{ox} (**5**) and DTT^{red} (**6**) suggested that DHS^{ox} (**2**) is a strong oxi-

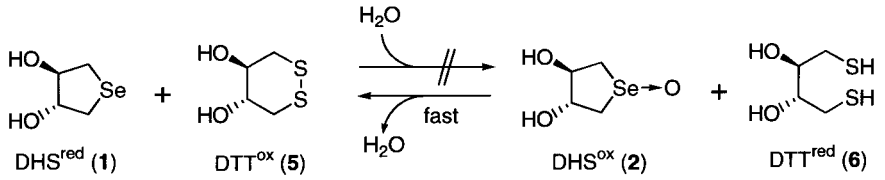

SCHEME 3

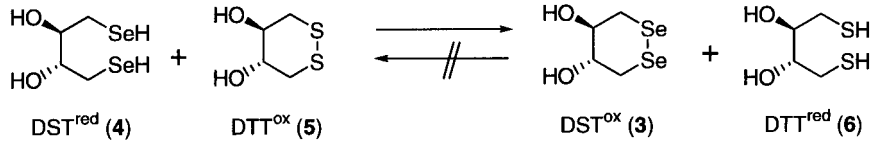

SCHEME 4

dizing agent for formation of protein SS bonds, while DST^{red} (**4**) is a strong reducing agent for cleavage of protein SS bonds. Molecular design of redox reagents using selenium, instead of sulfur, could be an effective approach to the redox control of protein structures.

EXPERIMENTAL

General

Commercially available organic and inorganic reagents were used without further purification. Dichloromethane (CH_2Cl_2) was dried over calcium hydride and was distilled under nitrogen before use. Methanol (MeOH) was distilled under nitrogen. Other organic solvents were used without purification. Column chromatography was carried out by using Fuji Silysia BW-300 silica gel. NMR spectra were measured on a JEOL α500 spectrometer. Dimethyl selenide (δ 0 ppm) in $CDCl_3$ was used as an external standard for measurement of ^{77}Se NMR chemical shifts.

*Synthesis of DL-trans-3,4-dihydroxy-1-selenolane (DHS^{red}) (**1**)*

To a freshly prepared aqueous solution of NaHSe [21] (19 mmol), 1,3-butadiene diepoxide (1.2 mL, 16 mmol) was added. The mixture was stirred for 10 minutes at room temperature under nitrogen and then overnight under air. The resulting mixture was filtered. The filtrate was extracted with ether for 3 days by using a liquid/liquid continuous extractor. Selenolane **1** was obtained from the ether layer by concentration and was purified by silica gel column chromatography (ether) or recrystallization from $CHCl_3$. Yield, 1.44 g (55%). Colorless crystals, m.p. 79–80°C. Spectral data for **1**: ^{1}H NMR (500 MHz in $CDCl_3$) δ 2.10 (d, J = 5.0, 2H), 2.87 (dd, J = 4.0 and 11.0, 2H), 3.16 (dd, J = 4.0 and 11.0, 2H), 4.27 (m, 2H); ^{13}C NMR (125.65 MHz) δ 26.8, 78.9; ^{77}Se NMR (95.35 MHz) δ 65.6. Anal. Calcd for $C_4H_8O_2Se$: C, 28.76; H, 4.83. Found: C, 28.55; H, 4.70.

*Synthesis of DL-trans-3,4-dihydroxy-1-selenolane oxide (DHS^{ox}) (**2**)*

To a CH_2Cl_2 solution (10 mL) of **1** (55 mg, 0.33 mmol), *m*-chloroperbenzoic acid (56 mg, 0.33 mmol) dissolved in CH_2Cl_2 (10 mL) was added slowly. Precipitated white crystals were collected by filtration. Obtained **2** was purified by recrystallization from MeOH. Yield, 41 mg (69%). Colorless crystals, m.p. 124–125°C. Spectral data for **2**: ^{1}H NMR (500 MHz in MeOH-d_4) δ 2.87 (d, J = 13.0, 1H), 3.08 (dd, J = 3.0 and 12.0, 1H), 3.58 (dd, J = 5.5 and 13.0, 1H), 3.78 (dd, J = 2.5 and 12.0, 1H), 4.63 (m, 1H), 4.72 (dd, J = 3.0 and 5.5, 1H), 4.80 (s, 2H); ^{13}C NMR (125.65 MHz) δ 55.0, 58.0, 79.1, 79.5; ^{77}Se NMR (95.35 MHz) δ 941.8. Anal. Calcd for $C_4H_8O_3Se$: C, 26.24; H, 4.41. Found: C, 26.16; H, 4.17.

*Synthesis of DL-trans-1,2-diselenane-4,5-diol (DST^{ox}) (**3**)*

To a freshly prepared aqueous solution of Na_2Se_2 [21] (38 mmol), 1,3-butadiene diepoxide (1.5 mL, 19 mmol) was added. The mixture was refluxed for 1 hour under nitrogen. The resulting mixture was then stirred overnight at room temperature under air. Selenium precipitates were filtered off. The filtrate was extracted with ether for 3 days by liquid/liquid continuous extraction. Diselenane **3** was obtained from the ether layer by concentration and was purified by silica gel column chromatography (ether) or recrystallization from MeOH. Yield, 2.54 g (54%). Yellow

crystals, m.p. 116–118°C. Spectral data for **3**: ^{1}H NMR (500 MHz in DMF-d_7) δ 3.16 (dd, J = 10.0 and 12.0, 2H), 3.43 (dd, J = 2.8 and 12.0, 2H), 3.53 (m, 2H), 5.20 (d, J = 4.0, 2H); ^{13}C NMR (125.65 MHz) δ 31.8, 75.4; ^{77}Se NMR (95.35 MHz) δ 268 (broad). Anal. Calcd for $C_4H_8O_2Se_2$: C, 19.53; H, 3.28. Found: C, 19.59; H, 3.14.

*Synthesis of DL-threo-2,3-dihydroxy-1,4-butanediselenol (diselenothreitol, DST^{red}) (**4**)*

To the yellow solution of **3** (69 mg, 0.28 mmol) in MeOH (0.5 mL), $NaBH_4$ was added under a nitrogen atmosphere until the solution color disappeared. Six milliliters of 6 M HCl was added to the solution. The resulting solution was then combined with 80 mL of ether and was stirred vigorously under nitrogen for 1 hour to extract **4** in ether. The ether layer was collected by using a syringe. The extraction was carried out two times. The combined ether layer was dried over $MgSO_4$. After decantation and concentrated under reduced pressure, **4** was obtained as a white powder. Diselenol **4** was air sensitive and contained ~20% of an unknown byproduct (^{77}Se NMR δ −82.8). Spectral data for **4**: ^{1}H NMR (500 MHz in $CDCl_3$) δ −0.51 (t, J = 7.5, 2H), 2.82 (m, 6H), 4.27 (m, 2H); ^{13}C NMR (125.65 MHz) δ 22.6, 80.7; ^{77}Se NMR (95.35 MHz) δ −78.3 (d, $^1J_{SeH}$ = 33.5).

*X-Ray Analysis of DHS^{red} (**1**)*

A Rigaku AFC6S diffractometer was employed with the Mo Kα (λ = 0.71073 Å) radiation monochromatized by graphite. Intensity data were collected using an ω-2θ scan technique to a maximum 2θ value of 60.0°. A total of 2674 reflections was collected. The structure was solved by the direct method (SIR-92) [22]. The final full-matrix least-squares refinement of F^2 against all unique 2596 reflections (R_{int} = 0.0745) was performed by using the SHELXL-97 program [23]. The crystal data obtained are as follows: Formula, $C_4H_8O_2Se$; M, 167.06; Space group, monoclinic C2/c (no. 15); a, 17.052(4) Å; b, 10.237(3) Å; c, 11.658(3) Å; β, 119.055(13)°; V, 1778.9(8) Å^3; Z, 12; μ, 6.2 mm^{-1}; D_c, 1.871 g/mL; T, 296 K; Size, 0.50 × 0.40 × 0.40 mm; Number of variables, 144; $R(F^2)$, 11.93; $wR(F^2)$, 13.88. The graphical molecular structure of **1** (Figure 1) was drawn using the ORTEP-3 program for Windows [24]. Complete lists of atomic coordinates, thermal parameters, and bond parameters have been deposited at the Cambridge Crystallographic Data Centre (No. CCDC-154248).

*X-Ray Analysis of DHS^{ox} (**2**)*

A Rigaku AFC6S diffractometer was employed with the Mo Kα (λ = 0.71073 Å) radiation monochromatized by graphite. Intensity data were collected using an ω-2θ scan technique to a maximum 2θ value of 55.0°. A total of 2629 reflections was collected. The structure was solved by the direct method (SIR-92) [22]. The final full-matrix least-squares refinement of F^2 against all unique 1358 reflections (R_{int} = 0.0466) was performed by using the SHELXL-97 program [23]. The crystal data obtained are as follows: Formula, $C_4H_8O_3Se$; M, 183.06; Space group, monoclinic *Pbca* (no. 61); a, 9.791(12) Å; b, 17.123(6) Å; c, 7.049(6) Å; V, 1181.8(18) Å^3; Z, 8; μ, 6.3 mm^{-1}; D_c, 2.058 g/mL; T, 296 K; Size, 0.40 × 0.40 × 0.30 mm; Number of variables, 105; $R(F^2)$, 7.29; $wR(F^2)$, 12.24. The graphical molecular structure of **2** (Figure 2) was drawn using the ORTEP-3 program for Windows [24]. Complete lists of atomic coordinates, thermal parameters, and bond parameters have been deposited at the Cambridge Crystallographic Data Centre (No. CCDC-154249).

*X-Ray Analysis of DST^{ox} (**3**)*

A Rigaku AFC6S diffractometer was employed with the Mo Kα (λ = 0.71073 Å) radiation monochromatized by graphite. Intensity data were collected using an ω-2θ scan technique to a maximum 2θ value of 55.0°. A total of 3163 reflections was collected. The structure was solved by the direct method (SIR-92) [22]. The final full-matrix least-squares refinement of F^2 against all unique 1584 reflections (R_{int} = 0.0459) was performed by using the SHELXL-97 program [23]. The crystal data obtained are as follows: Formula, $C_4H_8O_2Se_2$; M, 246.02; Space group, monoclinic $P2_1/a$ (no. 14); a, 8.386(3) Å; b, 8.5483(19) Å; c, 9.9690(18) Å; β, 105.06(2)°; V, 690.1(3) Å^3; Z, 4; μ, 10.6 mm^{-1}; D_c, 2.368 g/mL; T, 296 K; Size, 0.40 × 0.30 × 0.30 mm; Number of variables, 105; $R(F^2)$, 5.91; $wR(F^2)$, 9.63. Although numerical absorption corrections were recommended for this crystal [μ × size(mid) > 3.0], psi-scan corrections were applied due to technical difficulty in the numerical corrections. Resulting bond parameters (bond lengths, bond angles, and dihedral angles) were consistent with the normal values, except for the short bond length between O1 and H1 (0.67 Å) The graphical molecular structure of **3** (Figure 3) was drawn using the ORTEP-3 program for Windows [24]. Complete lists of atomic coordinates, thermal parameters, and bond parameters have been deposited at the Cambridge Crystallographic Data Centre (No. CCDC-154250).

Reactions of DHS or DST with DTT

For the reactivity tests, reverse-phase HPLC or NMR analysis was applied; 0.1 M stock solutions of DHS^{red}

(**1**), DHS^{ox} (**2**), DTT^{ox} (**5**), and DTT^{red} (**6**) and a 0.05 M stock solution of DST^{ox} (**3**) dissolved in degassed 0.1 M acetic acid were prepared. Two stock solutions, for example DHS^{red} and DTT^{ox}, were mixed in a buffer solution (a sodium acetate buffer at pH 4.0, a phosphate buffer at pH 7.0, or a tris buffer at pH 9.0) at various ratios. The dilution ratio was ~1000. The reaction mixture was then analyzed by use of a Hewlett Packard HP1100 Series HPLC system equipped with a Hewlett Packard ODS Hypersil column (4 × 125 mm). The system was equilibrated with 0.09% trifluoroacetic acid at the flow rate of 0.5 mL/min. After sample injection, a gradient was applied by increasing the ratio of acetonitrile, containing 0.09% trifluoroacetic acid, from 0 to 15% in 25 minutes. For the reaction between DST^{red} (**4**) and DTT^{ox} (**5**), DST^{red} prepared according to the aforementioned procedure was dissolved in D_2O and the solution was added with DTT^{ox}. NMR spectra of the mixture was then measured. Formation of DST^{ox} (**3**) and DTT^{red} (**6**) was clearly observed in the ^1H and ^{13}C NMR spectra.

REFERENCES

[1] (a) Gilbert, H. F. Avd Enzymol 1990, 63, 69–172; (b) Creighton, T. E. Biol Chem 1997, 378, 731–744.
[2] Anfinsen, C. B. Science 1973, 181, 223–230.
[3] Wedemeyer, W. J.; Welker, E.; Narayan, M.; Scheraga, H. A. Biochemistry 2000, 39, 4207–4216.
[4] Szajewski, R. P.; Whitesides, G. M. J Am Chem Soc 1980, 102, 2011–2026.
[5] Weissman, J. S.; Kim, P. S. Science 1991, 253, 1386–1393.
[6] Konigsberg, W. Methods Enzymol 1972, 25, 185–188.
[7] (a) Kuwajima, K.; Ikeguchi, M.; Sugawara, T.; Hiraoka, Y.; Sugai, S. Biochemistry 1990, 29, 8240–8249; (b) Ewbank, J. J.; Creighton, T. E. Biochemistry 1993, 32, 3677–3693; (c) Lees, W. J.; Whitesides, G. M. J Org Chem 1993, 58, 642–647.
[8] Cappel, R. E.; Gilbert, H. F. J Biol Chem 1986, 261, 15378–15384.
[9] Annis, I.; Chen, L.; Barany, G. J Am Chem Soc 1998, 120, 7226–7238.
[10] Shi, T.; Rabenstein, D. L. J Am Chem Soc 2000, 122, 6809–6815.
[11] Iwaoka, M.; Tomoda, S. Chem Lett 2000, 1400–1401.
[12] (a) Back, T. G., Ed. Organoselenium Chemistry: A Practical Approach; Oxford University Press: Oxford, 1999; (b) With, T., Ed. Organoselenium Chemistry: Modern Developments in Organic Synthesis; In Topics in Current Chemistry; 2000, Vol. 208.
[13] (a) Ogawa, A.; Nishiyama, Y.; Kambe, N.; Murai, S.; Sonoda, N. Tetrahedron Lett 1987, 28, 3271–3274; (b) Iwaoka, M.; Tomoda, S. J Am Chem Soc 1994, 116, 2557–2561.
[14] Preliminary results were reported in Ref. [1].
[15] (a) Cleland, W. W. Biochemistry 1964, 3, 480–482; (b) Carmack, M.; Kelley, C. J. J Org Chem 1968, 33, 2171–2173.
[16] Klapötke, T. M.; Broschag, M. Compilation of Reported ^{77}Se NMR Chemical Shifts: Up to the Year 1994; John Wiley & Sons: Chichester, 1996.
[17] (a) Clegg, W. Acta Crystallogr 1975, B31, 2722–2724; (b) Benz, G.; Born, L.; Brieden, M.; Grosser, R.; Kurz, J.; Paulsen, H.; Sinnwell, V.; Weber, B. Liebigs Ann Chem 1984, 1408–1423; (c) Nawata, Y.; Ishitani, Y.; Matsuura, I.; Oishi, H.; Ando, K. Acta Crystallogr 1989, C45, 1112–1113; (d) Rao, A. V. R.; Reddy, K. A.; Srinivas, N. R.; Gurjar, M. K.; Padmaja, N.; Ramakumer, S.; Viswamitra, M. A.; Swapra, G. V. T.; Jagannadh, B.; Kunwar, A. C. J Chem Soc Perkin Trans 1 1993, 1255–1259.
[18] Capasso, S.; Zagara, A. Acta Crystallogr 1981, B37, 1437–1439.
[19] Foss, O.; Johnsen, K.; Reistad, T. Acta Chem Scand 1964, 18, 2345–2354.
[20] (a) Karplus, M. J Chem Phys 1959, 30, 11–15; (b) Karplus, M. J Phys Chem 1960, 64, 1793–1798; (c) Karplus, M. J Am Chem Soc 1963, 85, 2870–2871.
[21] Klayman, D. L.; Griffin, T. S. J Am Chem Soc 1973, 95, 197–199.
[22] Altomare, A.; Cascarano, G.; Giacovazzo, C.; Guagliardi, A.; Burla, M. C.; Polidori, G.; Camalli, M. J Appl Crystallogr 1994, 27, 435–436.
[23] Sheldrick, G. M. SHELXL97: Program for the Refinement of Crystal Structures; University of Götlingen: Götlingen, Germany, 1997.
[24] Farrugia, L. J. ORTEP-3 for Windows, version 1.03; University of Glasgow: Glasgow, Scotland, 1997.